Fourier transform microwave spectrum of the propane–water complex: A prototypical water-hydrophobe system

D. W. Steyert,[a] M. J. Elrod, and R. J. Saykally
Department of Chemistry, University of California, Berkeley, California 94720

F. J. Lovas and R. D. Suenram
Molecular Physics Division, National Institute of Standards and Technology, Gaithersburg, Maryland 20899

(Received 17 March 1993; accepted 3 August 1993)

The Fourier transform microwave spectrum of the propane–water complex (C_3H_8–H_2O) has been observed and analyzed. This spectrum includes transitions assigned to propane complexed with both the *ortho* and *para* nuclear spin confirmations of water. The rotational constants indicate that the vibrationally averaged structure has all four heavy atoms coplanar, with the water center of mass lying on or near the C_2 axis of propane, inside the CCC angle, 3.76($\pm$0.02) Å from the propane center-of-mass, and 4.35($\pm$0.02) Å from the methylene carbon. The projection of the electric dipole onto the *a* inertial axis of the complex (0.732 D for the *ortho* state and 0.819 D for the *para* state) indicates that one of the protons of the water subunit lies on the C_2 axis of the propane monomer, which is also the axis connecting the subunit centers of mass. The small projection of the dipole along the *b* axis (0.14 D for the *ortho* state and 0.38 D for the *para* state) is most consistent with an equilibrium structure in which all three atoms of the water lie in the CCC plane of propane, with torsional tunneling about the hydrogen bond occurring on the same time scale as the overall rotation. The small internal rotation tunneling splittings that occur in the rotational spectrum of the propane monomer are not observed in the spectrum of the complex.

I. INTRODUCTION

The "hydrophobic interaction" is of great importance in chemistry, biology, and engineering, and has been the subject of a large number of studies.[1–5] While the strong water–water hydrogen-bonding interactions certainly provide the principal driving force for hydrophobic interactions, important effects are also attributable to the water–hydrophobe potentials. Very little experimental information currently exists for reliably characterizing the interaction between water and highly hydrophobic species, in particular, the saturated hydrocarbons. In this direction we have begun to apply Fourier transform microwave spectroscopy and far-infrared laser vibration–rotation–tunneling Spectroscopy (FIR-VRTS) to water–hydrophobe complexes with the goal of ultimately obtaining the relevant potential surfaces—a method which has been successfully demonstrated for the most simple water–hydrophobe prototype, ArH_2O.[6]

Legon and Millen[7] provide a set of generalizations for predicting the geometries of clusters containing hydrogen halides bonded to many molecules, deduced from the results of microwave spectroscopy studies. Hydrogen halides always act as Lewis acids, and usually approach the bonding partner from a direction in which a classic lone pair is directed. Furthermore, in the bonding of hydrogen halides to molecules which contain a pi bond instead of a lone pair, something resembling a hydrogen bond will form with the hydrogen halide acting as a proton donor and the region of highest electron density in the pi bond acting as the acceptor. In the cyclopropane–HF cluster, which has all four heavy atoms coplanar, the HF bonds to the midpoint of the strained C–C bond, apparently interacting with the electron density accumulated there by the ring strain.[8] In similar clusters, water can act as either the acid or as the base.[9] In complexes with acids (defined broadly enough to include even acetylene)[10] the hydrogen of the donor molecule approaches the water oxygen along the direction of one of the lone pairs. In another set of water-containing complexes, the water acts as the Lewis acid, with one hydrogen directly involved in hydrogen bonding to the electron-rich region of the acceptor, while the other hydrogen is essentially free.

It is quite remarkable that such a large number of the complexes studied to date have ground-state structures that are directly predictable from simple notions of hydrogen bonding, and yet the set of rules outlined above does not cover the case for which there is not a region of high electron density, either through a lone pair, a pi bond, or a strained sigma bond. In all practicality, the notion of a hydrogen bond has already been overextended by the attempted application to the bonding between water and unsaturated and strained-ring hydrocarbons, so it is not surprising that these guidelines are not particularly applicable to the bonding of water to saturated hydrocarbons. In fact, despite the widespread importance of hydrophobic interactions, there is relatively little investigation of complexes containing water or the hydrogen halides with partners that do not have lone pairs, pi bonds, or strained sigma bonds. Besides the water–methane,[11,12] and methane–

[a]Present address: Department of Chemistry and Physics, Beaver College, Glenside, PA 19038.

 0021-9606/93/99(10)/7424/7/$6.00

HCl[13] complexes, the only other such examples are studies of hydrocarbon–rare gas complexes.[14]

In an effort to address this deficiency, we present the results of an investigation of the microwave spectrum of the propane–water complex. In Sec. II the details of the apparatus and experimental technique are given, in Sec. III is a discussion of the spectrum and its assignment, and in Sec. IV is a discussion of the results obtained in terms of deducing the equilibrium structure and long time-scale dynamics of the complex. In the accompanying paper,[15] we describe our study of the far-infrared VRT spectrum of this propane–water complex.

II. EXPERIMENT

In order to determine the ground-state spectroscopic constants of this novel and interesting complex, the microwave spectrum was recorded in a pulsed supersonic expansion. The NIST Fourier transform microwave spectrometer has been described previously.[16,17] A 1% mixture of propane in argon was expanded supersonically through a pulsed molecular beam valve fitted with a unique front end plate containing a reservoir which holds 1–2 cm^3 of liquid.[18] The gas pulse expanded into the large vacuum chamber at 10^{-6} Torr and was probed by a microwave pulse optimized in power and duration to yield the maximum signal strength for the first observed transitions. Following the probe pulse, the emission signal from the cavity was digitized at intervals of 0.5 μs for a total of 256 μs. This time-domain signal was then Fourier transformed to yield a spectrum in the frequency domain. Typically 200–1000 nozzle pulses were averaged to obtain the final frequency measurements of the transitions.

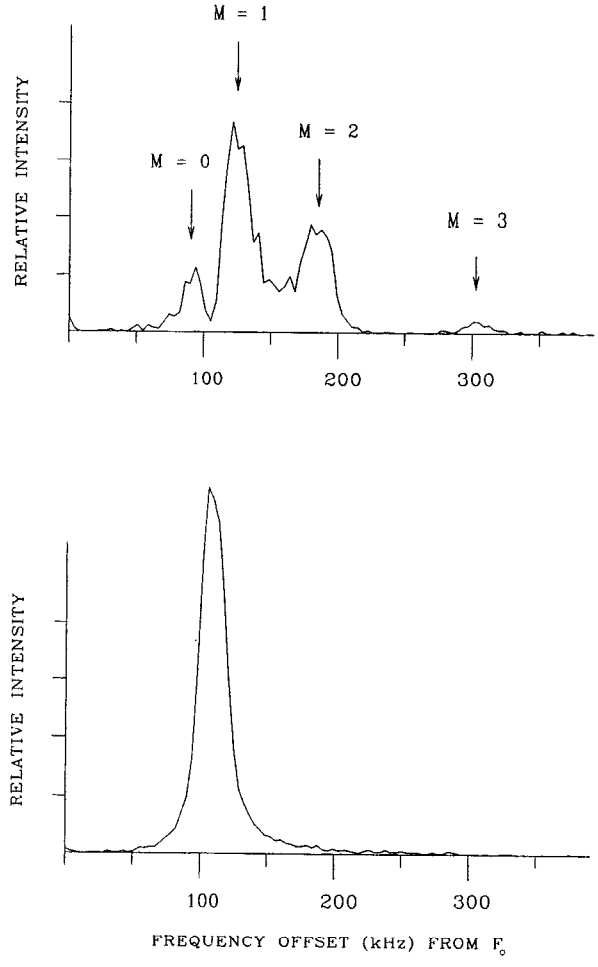

FIG. 1. The Stark effect on the 17.564 GHz microwave transition, lower trace: field off; upper trace: field on. Intensities are not accurate because the Stark pattern is wide compared to the cavity resonance, nonetheless, all four lobes are visible.

III. RESULTS

Guided by structural predictions and preliminary constants characterizing the spacing of the lines found in the best rigid-rotor patterns of the far-infrared VRT spectrum (see the accompanying paper),[15] the region near 17.5 GHz was initially scanned. This region was expected to have rotational transitions for a wide range of structural possibilities. The transitions actually found in this region, all of them weak singlets, were split into four components that tuned rather slowly when a Stark field, (chosen so that $\Delta M=0$ selection rules were obeyed, see Fig. 1) was applied. This is consistent with the second-order Stark effect typically found for the $J=4\leftarrow 3$ transitions of a molecule with nondegenerate energy levels. A typical absorption (the $4_{04}\leftarrow 3_{03}$ transition) is shown in Fig. 1, both with and without the application of the Stark field.

Subsequent scanning in this region and in the region between 12 and 13 GHz ($J=3\leftarrow 2$ transitions) revealed a sufficient number of transitions to allow the determination of the molecular constants of the VRT state which will be identified as the *ortho* nuclear spin confirmation of water in the subsequent discussion. From this fit, the remainder of the *a*-type rotational transitions were observed in the spectral region accessible with the spectrometer in its current configuration (9–18 GHz). Eventually, transitions involving states with $J=1$ through 4, $K_a=0$ through 2 were observed. Attempts to measure transitions between states with $K_a=3$ (with lower states almost 3 cm^{-1} above the $J=0$ level) were unsuccessful, as is typical for the 1 K molecular beam temperature produced with this instrument. Figure 2 shows a stick spectrum plot of all the observed transitions. The spectroscopic constants of the *ortho* state are given in Table I. The Hamiltonian for this work was expressed in terms of Watson's *S*-reduced parameters.[19]

It was clear from the early scans that the spectrum was more dense than expected for a simple semirigid rotor. The lines were tentatively grouped according to whether they were "strong" (*ortho*) or "weak" (*para*). Once all the transitions assigned to the *ortho* state were eliminated, the remaining transitions were assigned to the *para* state spectrum. These transitions could also be interpreted in terms of a semirigid Hamiltonian. In this case, however the weaker intensity prevented observation of the higher-energy $K_a=2$ states, even though they were well predicted. This spectrum is also shown in Fig. 2, and the fit to these data is presented in Table II. It should be noted that the

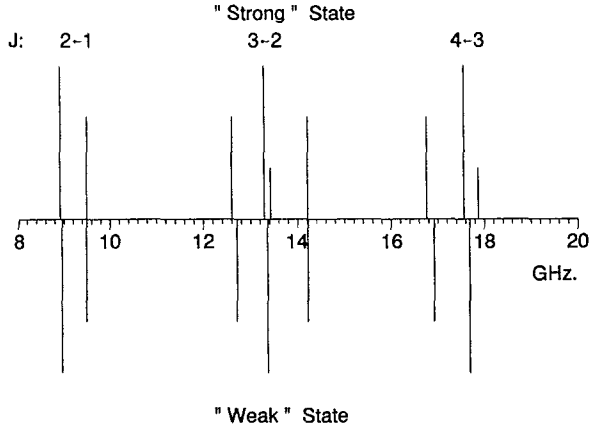

FIG. 2. A stick spectrum summarizing the microwave spectrum of propane–water. The lines are grouped according to whether they were assigned to the strong (*ortho*) or weak (*para*) state. Intensities are not accurate, but are intended to identify the value of K_a in the lower and upper state.

constants obtained from both the *ortho* and *para* fits are not as reliable as the uncertainties indicate due to correlations in the minimally determined data set. The combined FIR/MW fit reported in the following paper is much more reliable due to the much larger data set available.

The Stark effect on the microwave spectrum permitted a direct determination of the projection of the electric dipole moment onto the principal axes of the cluster. If the rotational constants of the cluster are known, one can predict the Stark shifts of the individual transitions as a function of electric field, which will be of the form

$$\nu=\nu_0+C_2E^2. \tag{1}$$

The observed frequencies of the Stark components were fit to this functional form, and the dipole moment projections adjusted in a least-squares fit to achieve good agreement between observed and calculated values for the C_2 coefficients.[20] These dipole moment projections are presented in Table III. The projection of the dipole on the *c* axis fit to a value near zero, and is so undetermined that it is assumed to actually be zero.

All the microwave transitions observed and assigned are *a* type; searches for transitions obeying *b*-type and *c*-type selection rules predicted from the fits of the *a*-type transitions of the *ortho* state were unsuccessful. No transitions were observed at the predicted frequencies, even with extensive signal averaging (3000 nozzle pulses, compared with the 50 pulses used for detecting the *a*-type transitions). The dipole moments presented in Table III indicate that weakly allowed *b*-type transitions should be present in the complex, but that they would be weaker by the ratio of the squares of the *a* and *b* dipoles, $(0.732/0.14)^2=27$.

TABLE I. Observed transitions, rotational constants, and derived constants of the *ortho* state of propane–water.

Transition	Frequency[a] (MHz)	Watson *S*-reduced constants[b,c]	
$2_{02}\leftarrow1_{01}$	8 918.654	A (MHz)	8441.7(3)
$2_{11}\leftarrow1_{10}$	9 490.991	B (MHz)	2507.667(2)
$3_{13}\leftarrow2_{12}$	12 600.302	C (MHz)	1969.306(2)
$3_{03}\leftarrow2_{02}$	13 290.925	D_J (kHz)	125.7(4)
$3_{22}\leftarrow2_{21}$	13 424.763	D_{JK} (kHz)	−136.6(1.2)
$3_{12}\leftarrow2_{11}$	14 213.021	D_K (kHz)	14.4(9)
$4_{14}\leftarrow3_{13}$	16 762.135	d_1 (kHz)	52.78(14)
$4_{23}\leftarrow3_{22}$	16 762.135	Δ^d μÅ^2	−4.74

[a]The estimated uncertainty in the frequency measurements is 4 kHz. The residuals resulting from the least-squares fit were within the estimated uncertainty.
[b]Values for additional distortion constants were set equal to zero.
[c]The numbers shown in parentheses are one standard deviation.
[d]$\Delta\equiv I_c-I_b-I_a$.

TABLE II. Observed transitions, rotational constants, and derived constants of the *para* state of propane–water.

Transition	Frequency[a] (MHz)	Watson *S*-reduced constants[b,c]	
$2_{02}\leftarrow1_{01}$	8 961.648	A (MHz)	8433.6(3)
$2_{11}\leftarrow1_{10}$	9 493.574	B (MHz)	2499.116(2)
$3_{13}\leftarrow2_{12}$	12 715.708	C (MHz)	1997.1596(16)
$3_{03}\leftarrow2_{02}$	13 366.241	D_J (kHz)	70.7(5)
$3_{12}\leftarrow2_{11}$	14 219.763	D_{JK} (kHz)	−64.4(6)
$4_{14}\leftarrow3_{13}$	16 920.277	d_1 (kHz)	26.2(3)
$4_{04}\leftarrow3_{03}$	17 683.606	Δ^d μÅ^2	−9.10

[a]The estimated uncertainty in the frequency measurements is 4 kHz. The residuals resulting from the least-squares fit were within the estimated uncertainty.
[b]Values for additional distortion constants were set equal to zero.
[c]The numbers shown in parentheses are one standard deviation.
[d]$\Delta\equiv I_c-I_b-I_a$.

IV. DISCUSSION

Three possible structural isomers for the propane–water complex are considered in Fig. 3. Comparing the separation between the center of mass of water and the nearest carbon to that observed in the methane–HCl complex (approximately 3.9 Å),[13] it is noted that for the "methylene-bonded" structure, the *B* constant would require an unrealistically close (3.39 Å, under a pseudodiatomic approximation) approach of the water to the central (methylene) carbon. In the other structure (called "kite-shaped") the separation of the center of mass of water from the end carbons [3.91(2) Å] is almost precisely the center-of-mass separation observed in methane–HCl. This particular configuration yields a pseudodiatomic center-of-mass separation of 3.76(2) Å. The distance between the water center of mass and the methylene carbon is found to be 4.35(2) Å.

TABLE III. Electric dipole components (D) of the propane–water van der Waals complex.

	Ortho state	*Para* state
μ_a	0.732(7)	0.819(62)
μ_b	0.14(1)	0.380(37)

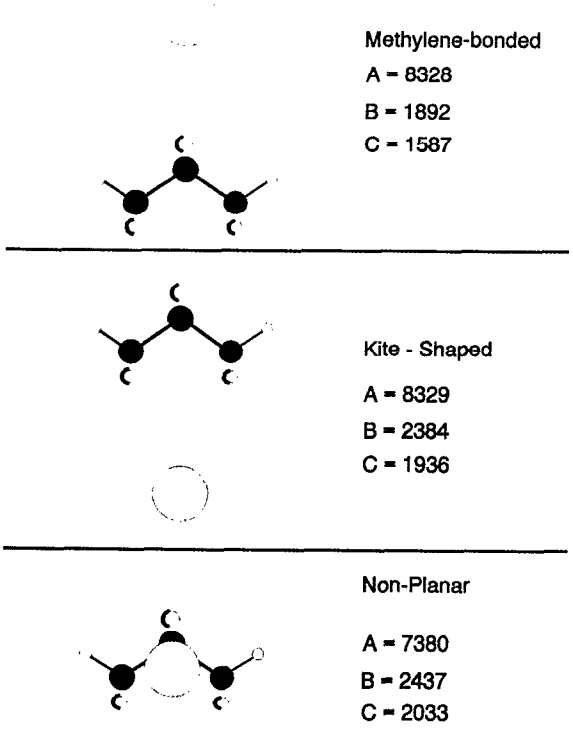

FIG. 3. Three conceivable structures for the complex, emphasizing the dependence of the rotational constants on structure. The orientation of the water (lightly shaded) is not specified because it has a very slight effect on the moments of inertia. To calculate the rotational constants (in MHz) of the complexes, the O–C bond length was assumed to be 3.76 Å. Note the discrepancy between the observed and structural values for *A*. Geometry of propane taken from Ref. 22.

Early calculations showed that a kite-shaped structural form could easily be adjusted to match the experimental *A* and *B* constants, especially if the water subunit were displaced slightly away from the C_2 axis of the propane subunit in the CCC plane. In no case, however, could the constant *C* be forced to match as well, without decreasing *B* significantly below the experimental value. The idea that the center of mass of the water molecule is displaced from the C_2 axis of the propane in the CCC plane suggests that there may be displacement away from that plane as well. This has the effect of rapidly decreasing *A*, while increasing *C* relative to *B*. Intuition suggests that there will be zero-point motion about some equilibrium structure that presumably has higher symmetry, and that if there is significant in-plane bending, there will also be significant out-of-plane bending. The fact that rigid-rotor moments of inertia calculated by slight displacements from the C_2 hydrogen-bonding geometry cannot simultaneously reproduce all three rotational constants argues that there must a large dynamical contribution to the rotational constants presented.

The presence of two low-lying states is easily rationalized by reference to the two nuclear spin states of water. Since there will be two orientations of the spin 1/2 nuclei (*ortho* and *para*), and since the total molecular wave function must correlate to water wave functions that are antisymmetric upon exchange of the protons, all molecular states correlating to the *ortho* state will have three times the statistical weight of the *para* state. Since collisional relaxation between the *ortho* and *para* manifolds is nuclear-spin forbidden, the populations will be "frozen" in a 3:1 ratio. Since the measured dipole moments of the strong and weak states are very similar, it follows that the relative strength of the two sets of microwave transitions must result from nuclear spin weights. Therefore, the strong and weak states are the two nuclear-spin configurations of the complex; the strong state correlates to the *ortho* states of water, and the weak state correlates to the *para* states of water.

The 100–600 kHz torsional tunneling splittings of uncomplexed propane[21] are easily resolved in the Fourier transform instrument of NIST, which has an accuracy of 4 kHz and a linewidth of about 15 kHz.[15] The microwave spectrum of the propane–water complex does not exhibit such small tunneling splittings, and there are two possible explanations: It is possible that the weak van der Waals interaction has served to increase the methyl internal rotation barriers such that tunneling is quenched. Repulsion between the methyl protons and the water molecule could act to significantly increase these barriers. However, the following discussion will show that the selection rules for the methyl internal rotor transitions are changed upon complexation with water such that the tunneling splitting cannot be directly measured, as is possible for free propane. The following discussion is based on Fig. 4. On the right side of that figure are the lowest rotational levels of propane,[21,22] corresponding to rotation about its *c* axis. To the left of that are the energy levels to be expected if the propane were artificially constrained to rotate only about its *b* (C_2 symmetry) axis. In this case the "rotational" energies would be given by

$$W = BK^2. \tag{2}$$

To the left of the diagram are the experimentally determined energy levels of the complex, and the significance of the artificial constraint now becomes clear. Free propane would be permitted to rotate about its *a* and *c* axes as well as the *b* axis, but upon complexation, these first two motions are quenched, and are replaced by rotation about the *b* and *c* principal axes, respectively, of the complex. Since the *b* axis of free propane becomes the *a* axis of the complex, each K_a stack of the complex correlates to a single rotational level of "constrained propane." This provides an explanation for the lack of tunneling splittings in the propane–water complex. Since all the observed microwave transitions were of *a* type, occurring between states in a given K_a stack, both energy levels in each microwave transition correlate to the same propane rotational level, and so all four tunneling transitions appear at essentially the same frequency, and detecting this splitting would require resolution well beyond the technology employed in the current study.

It is useful to compare the data assembled in this work with current knowledge regarding the methane–water complex.[11,12] This complex has been shown to have a dipole moment large enough to be detected easily in the

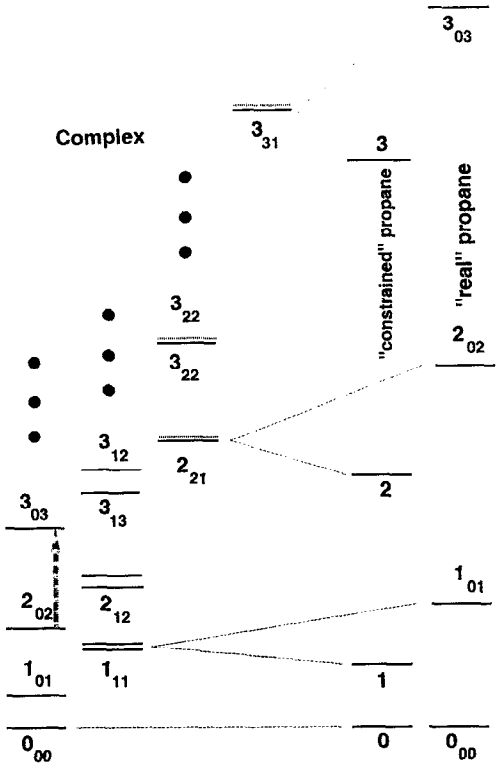

FIG. 4. A proposed correlation diagram for the propane subunit in propane–water. On the left of the diagram are some of the rotational energy levels of propane, and just to the right of that are the corresponding energy levels of propane artificially constrained to rotate about only the *b* axis. On the right are some of the energy levels of the propane–water complex. The arrow shows a typical transition of the microwave spectrum of the complex.

microwave[12] region. Because propane posesses low-order multipole moments[21,22] (dipole and quadrupole) that methane does not, it is expected that the propane–water system should exhibit larger and more anisotropic electrostatic attractive forces than those present in the methane–water system. In addition, the distinctly nonspherical electron density distribution of propane suggests that repulsive steric anisotropy will also act to constrain a propane-containing cluster more than the analogous methane-containing cluster. Both of these considerations suggest that propane–water should have a dipole moment at least as large as that of methane–water. Since propane–water does *not* have a large dipole moment, there must exist extensive vibrational averaging that serves to cancel out most of the *b*- or *c*-type dipole components.

At the logical extreme of this argument is a model which neglects zero-point vibration in all coordinates except the tunneling coordinate. We assume that the equilibrium structure places the water dipole, in the *a*–*b* plane, thereby projecting the total water dipole, 1.85 D,[23] onto the *a* and *b* molecular axes. Since the *ortho* state correlates to the $J=1$ level of the water subunit, and consequently has more extensive VRT motions to complicate the interpretation of the dipole moment projections, this elementary model best rationalizes the dipole moment projections for the *para* state, $\mu_A=0.819$ D, $\mu_B=0.380$ D. The dipole moment and polarizability of propane are negligible compared to the dipole of water, hence the *a*-type dipole is almost entirely due to the projection of the water dipole onto the *a* axis, so that the angle between the *a* axis of the complex and the dipole of the water, θ, is given by

$$\langle\cos\theta\rangle=\mu_A/\mu_{\text{water}}=0.819/1.85, \tag{3}$$

$$\langle\cos\theta\rangle=\cos\langle\theta\rangle, \tag{4}$$

$$\langle\theta\rangle=63.7^\circ, \tag{5}$$

where Eq. (4) above results from the assumed rigidity of the complex. In the above equations, the zero of θ is not specified, constrained only to lie on one or the other directions of the *a* axis, so intuition must guide this selection. If $\theta=0$ were chosen as the C_2 geometry with the water hydrogens farthest away from the propane subunit, then at $\theta=63.7^\circ$ the water assumes a very unlikely geometry, with one proton nearly on the complex *a* axis, but directed away from the propane subunit, and the other O–H bond in the heavy-atom (B–C) plane about 60° from the *a* axis, slightly toward the propane. This "anti-hydrogen-bonded" structure, although previously observed in FCl–FH,[8] seems unlikely, for it involves neither the O–H bond nor the oxygen lone pair in the bonding. On the other hand, if $\theta=0$ were the C_2 geometry with the hydrogens closest to the propane, $\theta=63.7^\circ$ would result in a structure entirely consistent with the structures of other water-containing complexes: One of the O–H bonds would be on or near the C_2 axis but closer to the propane, as shown in Fig. 5, which shows the equilibrium structure implied by these considerations.

The dipole moment projections also offer information about whether, on the time scale of the rotational experiments, there is a single average structure about which vibrational motion takes place. An inspection of the dipole moment projections, in particular the *b*-type dipole, casts doubt on this interpretation. In the linear "hydrogen-bonded" geometry, the dipole of the water would be pointed away from the molecular *a* axis at an angle of 52.5°, so that if the cluster were completely rigid, this would predict an *a* dipole, μ_A, and a *b* dipole μ_B given by

$$\mu_A=\mu_{\text{water}}\cos(52.5^\circ)=1.10\ \text{D}, \tag{6}$$

$$\mu_B=\mu_{\text{water}}\sin(52.5^\circ)=1.44\ \text{D}. \tag{7}$$

Vibrational averaging could readily reduce μ_A from 1.10 D to the experimental value of 0.819 D, but the large discrepancy between calculated (1.44 D) and observed (0.380 D) μ_B dipole moments casts doubt on this deep-minimum model. If, on the other hand, the water were free to rotate about the O–H–propane hydrogen bond, then the dipole would be given by $\mu_{\text{water}}\langle P_1(\cos\alpha)\rangle$, where α is the torsion angle of the hydrogen bond. Since the potential surface is twofold symmetric in α, $\langle P_1(\cos\alpha)\rangle=0$. For this interpretation to be viable, it requires that the tunneling motion be on the time scale of the rotational period, so that averaging between the two equilibrium structures is partial, but not complete. The observation of a small *b*-type

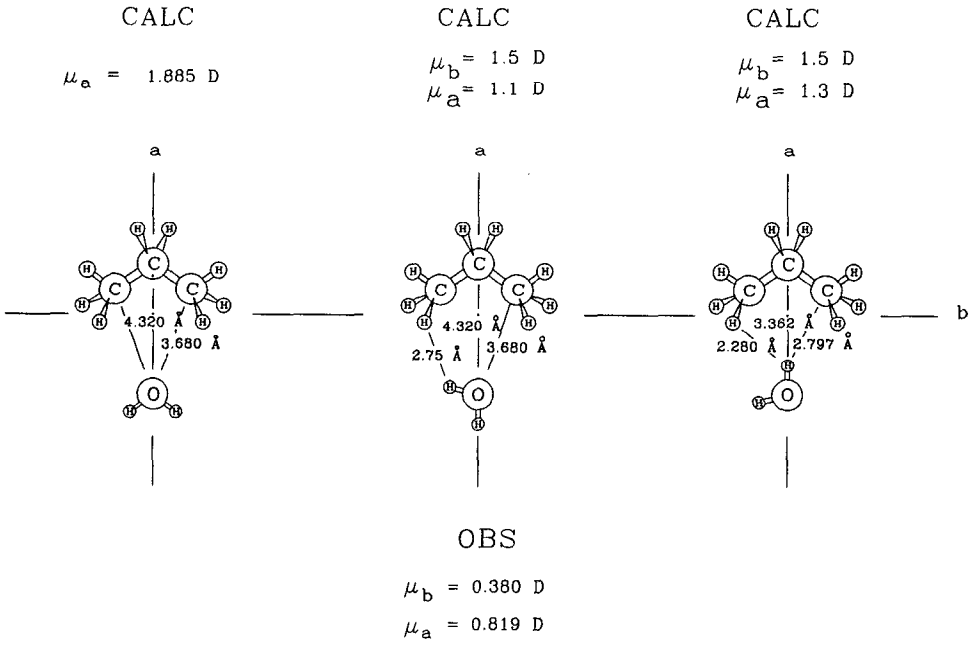

FIG. 5. Three conceivable structures of the propane–water complex, showing the dependence of the rotational constants and dipole on the location and orientation of water.

dipole can at least be rationalized in terms of this hydrogen-bonded structure, while it would be inconsistent with a C_2 symmetric average structure.

Yaron *et al.*[24] have used the dipole moments of *ortho* and *para* nuclear spin conformers of the complexes of water with carbon monoxide to deduce the geometry and the relative energy at the saddle point on the tunneling path. We can similarly explain our observation of a larger dipole moment for the *para* propane–water complex: Since the *para* state tunneling wave function must be symmetric, it does not have a node at the barrier and it has larger probability to be at the transition state. Thus, it exhibits a larger dipole moment. This suggests that the tunneling path involves rotation of water about its *b* axis. All observations are consistent with a C_{2v} transition state in which the three water atoms remain in the plane of the carbon atoms of propane.

V. CONCLUSIONS

This section is devoted to a qualitative rationalization for the propane–water bonding geometry and strength. As discussed in Sec. I, complexes involving water have been observed to bond principally along the sp^3 bonding axes of water, either along the O–H bond axis or along the lone pair. The propane–water complex apparently extends this trend, with water bonding to propane along the OH bond.

The orientation of the propane also deserves discussion. One could imagine the water occupying several other sites in the vicinity of the propane: As previously discussed, possible sites are: (1) on the C_2 axis of the propane, closer to the methylene carbon, (2) near either methyl carbon, with the van der Waals bond collinear with the CC bond, or (3) a position in which the water center of mass does not lie in the CCC plane of the propane.

Still another possible structure, proposed by Davis and Andrews[25] for the HF–propane complex has the HF interacting asymmetrically with one of the CC bonds from outside the CCC angle. Their matrix-isolation FTIR spectra indicate two distinct sites, and their *ab initio* calculations indicated a local minimum of energy with this structure. The present work and the work of Davis and Andrews suggest the rich complexity of possible structures to be observed in propane-containing clusters, and specifically, that multiple minima may also be observed for the propane-water system.

A more detailed characterization of the spectroscopy of this interesting system will be necessary before the relationship between this microwave structure and the potential energy surface can be completely understood. Another step in that direction is presented in the accompanying paper,[15] in which the measurement of a torsional vibration–rotation–tunneling band by tunable far-IR laser spectroscopy is presented.

ACKNOWLEDGMENTS

D.W.S., M.J.E., and R.J.S. are supported by the Experimental Physical Chemistry Program of the National Science Foundation (Grant No. CHE-9123335). Travel support for this collaboration was provided by the Graduate Division, University of California, Berkeley.

[1] L. R. Pratt and D. Chandler, J. Chem. Phys. **73**, 3434 (1980).
[2] W. C. Swope and H. C. Andersen, J. Phys. Chem. **88**, 6548 (1984).
[3] K. Watanabe and H. C. Andersen, J. Chem. Phys. **90**, 795 (1986).
[4] A. Ben-Naim, *Hydrophobic Interactions* (Plenum, New York, 1980).

[5] C. Pangali, M. Rao, and B. J. Berne, J. Chem. Phys. **71**, 2975 (1979).
[6] R. C. Cohen and R. J. Saykally, J. Chem. Phys. **98**, 6007 (1993).
[7] A. C. Legon and D. J. Millen, Faraday Discuss. Chem. Soc. **73**, 71 (1982).
[8] L. W. Buxton, P. D. Aldrich, J. A. Shea, A. C. Legon, and W. H. Flygare, J. Chem. Phys. **75**, 2681 (1981).
[9] T. R. Dyke, Topics Current Chem. **120**, 86 (1984).
[10] K. I. Peterson and W. Klemperer, J. Chem. Phys. **81**, 3842 (1984).
[11] L. Dore, R. C. Cohen, C. A. Schmuttenmaer, K. L. Busarow, M. J. Elrod, J. G. Loeser, and R. J. Saykally (unpublished).
[12] G. T. Fraser, R. D. Suenram, and F. J. Lovas (unpublished).
[13] Y. Oshima and Y. Endo, J. Chem. Phys. **93**, 6256 (1990).
[14] J. M. Hutson, Annu. Rev. Phys. Chem. **41**, 123 (1990).
[15] D. W. Steyert, M. J. Elrod, and R. J. Saykally, J. Chem. Phys. **99**, 7431 (1993).
[16] F. J. Lovas and R. D. Suenram, J. Chem. Phys. **87**, 2010 (1987).
[17] R. D. Suenram, F. J. Lovas, G. T. Fraser, J. Z. Gillies, C. W. Gillies, and M. Onda, J. Mol. Spectrosc. **137**, 127 (1989).
[18] F. J. Lovas, R. D. Suenram, G. T. Fraser, C. W. Gillies, and J. Zozom, J. Chem. Phys. **88**, 722 (1988).
[19] J. K. G. Watson, J. Chem. Phys. **46**, 1935 (1967).
[20] L. H. Coudert, F. J. Lovas, R. D. Suenram, and J. T. Hougen, J. Chem. Phys. **87**, 6290 (1987).
[21] F. J. Lovas and R. D. Suenram, J. Phys. Chem. Ref. Data **18**, 1245 (1989).
[22] D. R. Lide, Jr., J. Chem. Phys. **33**, 1514 (1960).
[23] P. W. Atkins, *Physical Chemistry*, 3rd ed. (Freeman, New York, 1986).
[24] D. Yaron, K. I. Peterson, D. Zolandz, W. Klemperer, F. J. Lovas, and R. D. Suenram, J. Chem. Phys. **92**, 7095 (1990).
[25] S. R. Davis and L. Andrews, J. Am. Chem. Soc. **109**, 4768 (1987).